JOURNAL OF VIROLOGY, May 2002, p. 4901–4911 Vol. 76, No. 10
0022-538X/02/$04.00+0 DOI: 10.1128/JVI.76.10.4901–4911.2002

Mechanism of Virulence Attenuation of Glycosaminoglycan-Binding Variants of Japanese Encephalitis Virus and Murray Valley Encephalitis Virus

Eva Lee* and Mario Lobigs

Division of Immunology and Cell Biology, John Curtin School of Medical Research, Australian National University, Canberra, ACT 0200, Australia

Received 14 December 2001/Accepted 8 February 2002

The in vivo mechanism for virulence attenuation of laboratory-derived variants of two flaviviruses in the Japanese encephalitis virus (JEV) serocomplex is described. Host cell adaptation of JEV and Murray Valley encephalitis virus (MVE) by serial passage in adenocarcinoma cells selected for variants characterized by (i) a small plaque phenotype, (ii) increased affinity to heparin-Sepharose, (iii) enhanced susceptibility to inhibition of infectivity by heparin, and (iv) loss of neuroinvasiveness in a mouse model for flaviviral encephalitis. We previously suggested that virulence attenuation of the host cell-adapted variants of MVE is a consequence of their increased dependence on cell surface glycosaminoglycans (GAGs) for attachment and entry (E. Lee and M. Lobigs, J. Virol. 74:8867–8875, 2000). In support of this proposition, we find that GAG-binding variants of JEV and MVE were rapidly removed from the bloodstream and failed to spread from extraneural sites of replication into the brain. Thus, the enhanced affinity of the attenuated variants for GAGs ubiquitously present on cells and extracellular matrices most likely prevented viremia of sufficient magnitude and/or duration required for virus entry into the brain parenchyma. This mechanism may also account, in part, for the attenuation of the JEV SA14-14-2 vaccine, given the sensitivity of the virus to heparin inhibition. A pronounced loss of the capacity of the GAG-binding variants to produce disease was also noted in mice defective in the alpha/beta interferon response, a mouse strain shown here to be highly susceptible to infection with JEV serocomplex flaviviruses. Despite the close genetic relatedness of JEV and MVE, the variants selected for the two viruses were altered at different residues in the envelope (E) protein, viz., Glu_{306} and Asp_{390} for JEV and MVE, respectively. In both cases the substitutions gave the protein an increased net positive charge. The close spatial proximity of amino acids 306 and 390 in the predicted E protein structure strongly suggests that the two residues define a receptor-binding domain involved in virus attachment to sulfated proteoglycans.

Altered virulence properties of viral variants are the basis for their application as live attenuated vaccines. Therefore, it is of particular interest to elucidate first the mechanisms for loss of the capacity of the variants to produce disease in a host and then the viral molecular determinants for the altered virulence phenotypes. Potential mechanisms for the attenuation of viral virulence include (i) changes in viral binding and penetration properties on host membranes resulting in altered tissue tropisms, (ii) a reduction of viral replication rate in vivo, (iii) a decreased efficiency of virus spread in the host, and (iv) an increased susceptibility of variant viruses to host antiviral responses (reviewed in reference 35). Virulence attenuation has traditionally been achieved by serial passage of virus in cultured cells or laboratory animals, a selection process that can give rise to adaptive changes that result in reduced virulence in the natural or incidental hosts. We report here on the mechanism for virulence attenuation of laboratory-derived encephalitic flavivirus variants with altered attachment and entry properties.

The flavivirus genus is a group of predominantly arthropod-borne positive-strand RNA viruses that can cause serious human diseases, such as yellow fever, dengue fever, and a number of viral encephalites (for a review, see reference 3). The most important mosquito-borne encephalitic flaviviruses are members of the Japanese encephalitis virus (JEV) serocomplex, a group of antigenically closely related viruses including JEV, Murray Valley encephalitis virus (MVE), West Nile virus, and St. Louis encephalitis virus (6). Members of the JEV serocomplex have a wide distribution and are maintained in a predominantly avian host-mosquito vector transmission cycle. Most human infections with these viruses are subclinical; the estimated ratio of inapparent to apparent infection is between 200:1 and 1,000:1. However, the case fatality rate can be as high as 50% and life-long neurological sequelae frequently occur among survivors of flaviviral encephalitis (for a review, see reference 3).

Mice are an excellent animal model for studying flaviviral encephalitis in humans. Similar to human infections, extraneural inoculation of JEV serocomplex viruses into adult mice is mostly associated with low or undetectable viremia and infrequent morbidity and mortality (10, 20). However, when injected directly into the brain, the viruses grow to high titers, causing a mostly fatal encephalomyelitis. Thus, the crucial but as-yet-unknown step leading to encephalitic disease in peripherally infected humans and mice appears to be a relatively rare stochastic event that permits virus in the circulation to breach the blood-brain barrier and enter the brain parenchyma.

* Corresponding author. Mailing address: Division of Immunology and Cell Biology, John Curtin School of Medical Research, Australian National University, P.O. Box 334, Canberra, ACT 2601, Australia. Phone: 61-2-61253526. Fax: 61-2-61252595. E-mail: Eva.Lee@anu.edu.au.

In mice, the resistance to extraneural infection with JEV serocomplex viruses is strictly age dependent (7, 8, 10, 20); until the age of 3 to 4 weeks the animals are susceptible to a low peripheral inoculum of virulent (neuroinvasive) virus strains. In these young mice, encephalitic flaviviruses can be detected in extraneural tissues and in the blood, allowing the kinetics of virus spread into the brain from the site of inoculation to be monitored (23, 25). Given their susceptibility to peripheral inoculation with neuroinvasive but not attenuated viruses of the JEV serocomplex, 3-week-old mice are routinely used in virulence determinations of virus isolates by comparing 50% lethal dose (LD_{50}) values after intraperitoneal (i.p.) and intracranial (i.c.) infection (17, 24).

Studies of the virulence attenuation of flaviviruses have provided much information in terms of the genetic changes that can give rise to altered virulence properties, but mostly in the absence of an understanding of the relevant in vivo mechanisms for attenuation. Two live, attenuated vaccines against flaviviruses are currently used for the immunization of humans against yellow fever or Japanese encephalitis. The yellow fever virus 17D vaccine strain is separated by 243 passages and 32 amino acid changes from the parental virus (9, 30). This multitude of genetic differences, as well as the likelihood that a number of properties of virus growth in the animal host distinguish the vaccine strain from the parent virus, has prevented identification of the molecular determinants and in vivo mechanisms for attenuation. The genetic complexity separating JEV strain SA14 and the vaccine derivative SA14-14-2 is less elaborate (27), but a comparison of the two viruses has also failed to reveal the mutation(s) and mechanism(s) that account for loss of neuroinvasiveness and reduced neurovirulence of the vaccine strain. However, other studies lend support to the importance of an amino acid substitution at position 138 (Glu to Lys) in the E protein of the SA14-14-2 virus in producing the attenuated phenotype, because variants with a single amino acid change at this position have growth and virulence properties comparable to those of the vaccine strain (5, 33).

Interestingly, the substitution at JEV E protein residue 138 also resulted in the increased binding affinity of the attenuated variants to sulfated glycosaminoglycans (GAGs) and the increased susceptibility of virus infectivity to inhibition with heparin (a soluble, highly sulfated GAG), in comparison to the virulent parent virus (32). GAGs are molecules ubiquitously expressed on the cell surface and extracellular matrix that are exploited by many different viruses in the attachment and entry process (31). The possibility of a causal relation between enhanced binding affinity to GAGs and virulence attenuation of flavivirus variants was first raised by us in a study of MVE variants with changes at E protein residue 390 located in the putative flavivirus receptor-binding domain (13) and later for host cell-adapted variants of tick-borne encephalitis virus (21). Attenuated variants of MVE with substitutions at E protein residue 390 and altered attachment and entry properties, reflected in an increased dependence on GAGs for infection of some host cells, were rapidly selected by adaptation to growth of the parent virus in a human adenocarcinoma cell line (SW13) (13, 17). Here we have extended the investigation of the effect of altered GAG-binding affinity on virulence attenuation to the medically more important encephalitic flavivirus, JEV, and characterized the mechanism for the reduced capacity of the host cell-adapted JEV and MVE variants to produce disease in mice.

MATERIALS AND METHODS

Cells. Vero (African green monkey kidney), SW13 (human adenocarcinoma), BHK-21 (baby hamster kidney), and C6/36 (*Aedes albopictus*) cells were obtained from the American Type Culture Collection and grown in Eagle's minimal essential medium plus nonessential amino acids (MEM) supplemented with 5% fetal calf serum (FCS) or 8% FCS for C6/36 cells. The vertebrate cells were grown at 37°C, and the insect cells were grown at 28°C.

Viruses. Working stocks of JEV, strain Nakayama (Jn) (16), are suckling mouse brain homogenates (10% in Hanks balanced salt solution [HBSS] containing 0.2% bovine serum albumin [BSA] and 20 mM HEPES [pH 8.0]; this medium is referred to here as HBSS-BSA). Plaque-purified stocks were prepared by picking plaques from Vero cell monolayers under agar overlay and amplifying once in Vero cells. Working stocks of JEV SA14 strain and its vaccine derivative SA14-14-2 (27) are kindly provided by Roy Hall, Department of Microbiology, University of Queensland, Brisbane, Queensland, Australia. Working stocks contained titers of 2×10^8 and 1.5×10^6 PFU/ml for SA14 and SA14-14-2, respectively. MVE strains MVE_{Asp390}, MVE_{His390}, MVE_{Gly390}, and MVE_{Ala390} are plaque-purified derivatives of the MVE full-length clone pM212 with a single amino acid alteration at residue 390 in the E protein as described previously (13). They share similar phenotypic properties of small plaque morphology, sensitivity of infectivity to heparin, and loss of neuroinvasiveness (13).

Mice. Swiss white outbred and alpha interferon-receptor knockout (IFN-α-$R^{-/-}$; C57BL/6 background [26]) mice were provided by the Animal Breeding Facility at the John Curtin School of Medical Research, Canberra, Australia, and maintained under specific-pathogen-free conditions.

Heparin inhibition assay. Monolayers of Vero, BHK-21, and SW13 cells in six-well plates (5×10^5 cells per well; Linbro) were either preincubated for 15 min with heparin in HBSS-BSA (50 or 200 μg/ml) or mock treated and then infected with ~200 PFU of virus, which was also pretreated with or without heparin (50 or 200 μg/ml), in a final volume of 100 μl in HBSS-BSA. Specific virus titers for each of the cell lines were determined by prior titration in the respective cells. Virus adsorption was for 1 h with regular rocking, and the inoculum was aspirated before the addition of agarose overlay medium containing MEM (JRH Biosciences, Lenexa, Kans.), 1% FCS, and 1% agar (Difco Laboratories, Irvine, Calif.). Monolayers were incubated at 37°C in a humidified chamber containing 5% CO_2 in normal air for 4 (Vero and BHK cells) or 5 (SW13 cells) days and then stained by the addition of 0.02% neutral red in HBSS (1 ml per well) on top of the agarose overlay for 16 h, or 0.1% crystal violet in 20% ethanol, after removal of the agarose overlay.

Inhibition of infectivity of JEV SA14 and SA14-14-2 viruses was examined by incubating virus (5×10^4 PFU) with heparin (50 and 200 μg/ml) for 15 min prior to its addition to BHK-21 and SW13 cell monolayers (10^5 cells/well in 24-well plates). Mock-treated controls were prepared by preincubation of the same amount of virus in HBSS-BSA in the absence of heparin. Supernatant virus was collected at 24 h postinfection (p.i.) and titrated by plaque formation on Vero cells under agarose overlay.

Nucleotide sequence analysis. Viral RNA from infected cells was sequenced as described previously (14). Briefly, total RNA was extracted from infected cells (36) for reverse transcription-PCR (RT-PCR) amplification to generate cDNA encoding the prM and E protein genes (nucleotides 564 to 2537 [22]). RT was performed by using Expand Reverse Transcriptase (Roche), RNAGuard (Pharmacia Biotech), random hexamers (Promega), and ~1 μg of total infected cell RNA according to the manufacturers' instructions. PCR products were gel purified (without exposure to UV irradiation) and sequenced by using an ABI Prism Big Dye Terminator Cycle Sequencing Ready Reaction Kit (Applied Biosystems) according to the manufacturer's instructions. Oligonucleotides used in RT-PCR and sequencing included the sense primers P564 (5′-AGAGGACG TGGACTGTTGGTGTGA-3′) and P964 (5′-AGCTGCTTGACAATTATG-3′) and the antisense primers P1316 (5′-GGTTTTCCGAAGTGGTGG-3′), P1716 (5′-AGGTGGCCTGATGTTAAC-3′), P2116 (5′-TGCCAGTCTTTGAGCTC C-3′), and P2516 (5′-CCTTGTGCGCTTTGTGGACGAT-3′).

Virulence assay. Virulence assays with 3-week-old Swiss white outbred mice were performed as described previously (17). Groups of five animals were inoculated with 30 μl of virus serially diluted in HBSS-BSA via the i.c. and i.p. routes. Mice were observed for 14 days for morbidity and mortality.

Assay for virus clearance. Clearance of virus from the bloodstream was assayed monitoring the intravenous (i.v.) inoculation of ~10^7 PFU of JEV or ~10^5 PFU of MVE strains into 8-week-old Swiss outbred mice. Blood was taken from the orbital plexus of animal under anesthesia at 5 min and 30 min p.i. and

allowed to clot at room temperature, and serum was collected for storage at −70°C. Virus titers in serum samples were determined by plaque titration on Vero cells and multiplied with an estimate of the blood volume of each animal as 7% of body weight (1).

Preparation of ^{35}S-radiolabeled virus. ^{35}S-labeled MVE and JEV was prepared by infection (multiplicity of infection of ~0.5) of BHK-21 cell monolayers in 15-cm^2 culture dishes (Nunc), starvation of cells at 24 h p.i. in MEM without cysteine and methionine (Gibco-BRL) for 30 min, and then replacement of growth medium with 8 ml of MEM with 1/20 of the normal concentration of cysteine and methionine, 2% FCS, and 10 μCi of [^{35}S]methionine (Amersham)/ml. Supernatant was collected at 48 h p.i., clarified by centrifugation at 4°C (8,000 × *g*) for 10 min, layered on top of a 10 to 30% sucrose gradient (31 ml) in NTE-BSA buffer (120 mM NaCl, 12 mM Tris-HCl [pH 8.0], 1 mM Na_2EDTA, 0.1% BSA), and centrifuged for 3 h at 26,000 rpm at 4°C in a SW28 rotor (Beckman). Fractions of ~1.4 ml each were collected from the bottom of the gradients, and virus peaks were identified by scintillation counting and then pooled. Gradient-purified virus was concentrated by using an Amicon Centricon-100 microconcentrator (Millipore), suspended in 1.5 ml of phosphate-buffered saline plus 0.1% BSA, and concentrated again in the microfiltration device; this process was repeated three times. The final concentrate (0.1 of 0.2 ml) was stored at −70°C.

Binding to heparin-Sepharose. Heparin-Sepharose beads (Pharmacia Biotech) were preequilibrated in a buffer containing10 mM sodium phosphate and 120 mM NaCl (pH 7.4). Binding of ^{35}S-labeled, gradient-purified MVE and JEV was performed in duplicate for 2 h at 4°C in microcentrifuge tubes in total volumes of 300 μl containing 50 μl of heparin-Sepharose and ~2 × 10^4 cpm of virus (10^3 to 10^4 PFU/cpm) with constant rotation. An excess amount of heparin-Sepharose was used for binding of the aliquots of radiolabeled virus to prevent saturation of binding. This was determined by performing a second-round incubation of unbound material with a fresh aliquot of heparin-Sepharose as described above, which gave negligible recovery of radioactivity. Sepharose beads were washed three times with a buffer containing 10 mM sodium phosphate, 120 mM NaCl (pH 7.4), and 0.1% BSA; resuspended in 50 μl of 1% sodium dodecyl sulfate–0.5 M NaCl–10 mM sodium phosphate (pH 7.4); and incubated at 65°C for 5 min to dissociate the bound virus. The supernatant was subjected to scintillation counting after the addition of a liquid scintillation cocktail (ReadyFlow III; Beckman Instruments, Inc.).

Organ distribution of radiolabeled virus after i.v. inoculation. Mice (6 weeks old) were inoculated i.v. with ^{35}S-labeled, gradient-purified MVE and killed by exsanguination under ether anesthesia after 30 min; the livers, spleens, lungs, and kidneys were then collected. Organs were finely diced with scissors and resuspended in 5 ml of 5 M NaOH and incubated at 70°C for 3 h, and the solution neutralized by the addition of glacial acetic acid. Aliquots (0.5 ml) were subjected to scintillation counting after the addition of 10 volumes of a liquid scintillation cocktail (ReadyFlow III).

Determination of virus titers in mouse tissues. Three-week-old Swiss white outbred mice in groups of three were inoculated with 1,000 PFU of JEV (30 μl in HBSS-BSA) in the left footpad. Blood was collected from the orbital plexus daily from 1 to 4 days p.i. and at the times of tissue collection. At 2, 4, 6, and 8 days p.i., mice were killed by cervical dislocation, and the livers, spleens, and brains were removed aseptically and snap-frozen immediately on dry ice. The tissues were processed as follows: brain, liver, spleen, and kidney tissues were finely diced with scissors, 9 volumes of HBSS-BSA was added, and homogenization was achieved by passing mixtures through a syringe with a succession of 18-, 21-, 23-, and 26-gauge needles attached. The homogenates were snap-frozen, thawed, clarified by centrifugation at 10,000 × *g* at 4°C, and stored in aliquots at −70°C for infectivity titration.

RT-PCR. For RT-PCR analysis, total RNA was extracted from each tissue (~20 mg) by a method modified from that described by Xie and Rothblum (36). Briefly, 0.5 ml of a solution containing guanidinium isothiocyanate (4 M), sodium citrate (25 mM), sodium acetate (0.2 M; pH 4.0), and β-mercaptoethanol (0.1 M) was added to the tissue sample, followed by vortexing for 1 min, the addition of 0.5 ml of acid-equilibrated phenol-chloroform-isoamyl alcohol (25:24:1; pH 4.7; Sigma), and further vortexing for 1 min at 4°C. Aqueous mixtures from each sample were collected after centrifugation at 28,000 × *g* for 10 min, mixed with an equal volume of ice-cold isopropanol, and held at −20°C for 30 min. RNA pellets were recovered by centrifugation at 28,000 × *g* for 15 min at 4°C, washed twice in 70% ice-cold ethanol, vacuum dried, and suspended in nuclease-free water (Sigma). RT-PCR was performed as described above with random hexamers for RT and primers P964 and P1316 for PCR.

RESULTS

Isolation of small-plaque variants of Jn by serial passage in human adenocarcinoma cells. Jn was serially passaged in SW13 cells to test whether variants with biological properties analogous to those of SW13 cell-adapted MVE could be obtained. These include an increased dependence on GAGs in the attachment and entry of host cells and the loss of neuroinvasiveness in mice (13). Variants of JEV were generated by five passages in SW13 cells, using as a starting material either an uncloned stock (giving rise to Js1, Js2, and Js3) or two plaque-purified virus stocks (giving rise to Js4 and Js5). The same plaque-purified Jn stock was also passaged five times in Vero cells to generate Jv1 after plaque purification. All SW13 cell-passaged viruses produced small plaques (~0.5 mm in diameter) on Vero and SW13 cell monolayers, in contrast to Jn and Jv1, which produced large plaques (3 to 4 mm and 1.5 to 2 mm on Vero and SW13 cell monolayers, respectively) after identical incubation periods. The small plaque phenotype of SW13 cell-passaged JEV was comparable to that observed for MVE variants adapted to growth in this cell line (13) and is likely the result of their greater sensitivity to the inhibitory effect on virus growth of sulfate impurities in the agar overlay, relative to that of Jn and Jv1.

Heparin sensitivity of SW13 cell-adapted JEV. Heparin is a highly sulfated proteoglycan structurally similar to heparan sulfate. It is a potent inhibitor of infectivity for many viruses which rely on GAGs in the attachment and entry process (2, 31). Heparin sensitivity assays were performed for the parental and passaged strains of JEV by preincubating virus inocula and cell monolayers with heparin and determining the effect on infectivity by plaque formation on Vero and SW13 cells. Heparin reduced plaque numbers of Jn and Jv1 viruses by 20 to 25% on Vero cells and ~65% on SW13 cells relative to mock-treated inocula (Fig. 1). The SW13 cell-passaged variants were significantly more sensitive to the inhibitory effects of heparin, which gave a reduction of infectivity of 74 to 91% on Vero and 97 to 99% on SW13 cell monolayers (Fig. 1).

GAG-binding properties of SW13 cell-passaged and parental viruses. The relative affinity for GAGs of SW13 cell-passaged and parental JEV was compared by using heparin-Sepharose and ^{35}S-labeled, gradient-purified virus. Binding of radiolabeled virus to heparin-Sepharose was performed over 2 h, and bound counts per minute were determined by scintillation counting after unbound virus was removed. Comparison between Jn and Js1 showed only ~15% of Jn bound to heparin-Sepharose and significantly more of Js1 (~40%) bound (Fig. 2). Similar binding assays were performed with a pair of MVE strains previously characterized in virulence and heparin sensitivity assays (13); MVE_{Asp390} is the MVE-1-51 strain derived from a full-length cDNA clone of MVE, whereas MVE_{Gly390} is an attenuated derivative of the full-length cDNA with an Asp-to-Gly substitution at residue 390 in the putative receptor-binding domain in the E protein that gives rise to an increased dependence on GAGs for virus attachment and entry and is associated with virulence attenuation (13). The Asp_{390} virus showed >2-fold less binding to heparin-Sepharose (13%) than the Gly_{390} variant (28%) (Fig. 2). The data are consistent with a stronger affinity of the heparin-sensitive

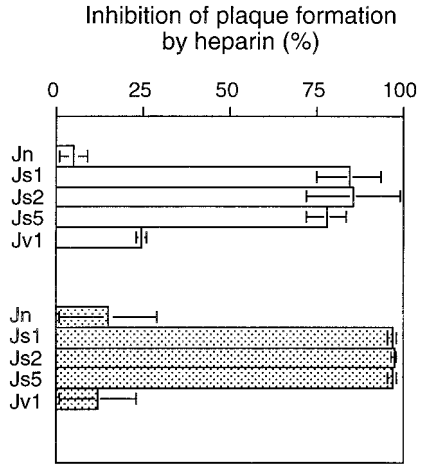

FIG. 1. Inhibition by heparin of infectivity of Jn and passaged viruses. Jn virus, SW13 cell-passaged viruses (Js1, Js2, and Js5), and Vero cell-passaged virus (Jv1) were incubated with heparin (200 μg/ml) for 15 min prior to their addition to Vero (open bars) and SW13 (gray bars) cell monolayers. Error bars show the standard deviation values calculated for each set of duplicates. The percent inhibition of plaque formation by heparin was calculated as follows: [(1 − plaque number in the presence of heparin)/plaque number for mock-treated control] × 100%.

strains of JEV and MVE to the negatively charged GAGs than that of the parental viruses.

Virulence attenuation of SW13 cell-passaged JEV. The virulence property of host cell-adapted and parental JEV was examined in 3-week-old Swiss outbred mice by the inoculation of 10-fold serial virus dilution via the i.c. and i.p. routes. Comparison of the i.c. and i.p. LD_{50} values (2.4 and 15.3 Vero cell PFU, respectively), which did not differ by more than 1 log, shows that Jn is highly virulent (Fig. 3A). In contrast, Js1 did not produce >25% mortality by the i.p. route even at the highest dose (10^5 PFU) despite an i.c. LD_{50} value of 1.1 Vero cell PFU (Fig. 3A). Thus, variant Js1 is attenuated due to the loss of neuroinvasiveness.

The neurovirulence of the SW13 cell-passaged JEV was not different from that of Jn according to the i.c. LD_{50} values and

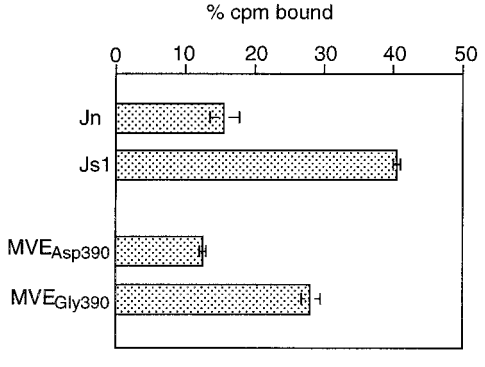

FIG. 2. Binding of parental and variant strains of JEV and MVE to heparin-Sepharose. ^{35}S-labeled, gradient-purified virus preparations were incubated with heparin-Sepharose, and the percent counts per minute bound were determined after 2 h at 4°C. The means for two samples ± the standard deviation are presented.

average survival times (5.6 ± 0.55 and 6.5 ± 1.05, respectively). This would suggest that growth of the passaged variant in brain tissues is not significantly restricted. This was further evaluated by infectivity assays performed with brain samples harvested at 2 days p.i. from 3-week-old Swiss outbred mice inoculated i.c. with 10^2 or 10^3 PFU of Jn or Js1. Both virus doses gave similar titers (~2×10^4 PFU/g) in Js1-infected mice ($n = 4$) demonstrating virus growth in the brain, albeit less rapid growth than that of Jn, which produced titers in the brain that were 10- to 1,000-fold higher (2×10^5 to 4×10^7 PFU/g; $n = 4$) than that of the passage variant.

Spread of SW13 cell-passaged and parental JEV in 3-week-old Swiss outbred mice. The mechanism for the loss of neuroinvasiveness of SW13 cell-passaged JEV was addressed by examining the kinetics of virus spread from an extraneural site of inoculation in comparison to that of the parental virus. Mice were inoculated in the footpad with 10^3 Vero cell PFU of Jn or Js1, and the brains, spleens, and livers were collected at 4, 6, 7, and 8 days p.i. For viremia determination, blood was also collected between 1 and 8 days p.i. Jn produced a detectable viremia at 2 and 3 days p.i. (Fig. 4A), which resulted in virus spreading into the brain, where high virus titers were observed 7 and 8 days p.i. (Fig. 4B). Low virus titers (0.5×10^3 to 1.0×10^3 PFU/g) were also present in the liver after day 6 p.i. (Fig. 4B), but virus was not detected in the spleen at any time point (data not shown). Mice inoculated with Js1 showed no viremia (Fig. 4A) and no infectious virus in the brain, liver, and spleen (Fig. 4B; data not shown) at any time, suggesting a loss of capacity of the variant to spread in the host from the site of footpad inoculation.

Spread of SW13 cell-passaged and parental JEV in 3-week-old IFN-α-$R^{-/-}$ mice. Knockout mice defective in the function of the IFN-α receptor (IFN-α-$R^{-/-}$ mice) are completely unresponsive to IFN-α/β (26) and highly susceptible to extraneural infection with JEV serotype flaviviruses (our unpublished results). Given the relatively poor growth even of the virulent Jn virus in extraneural tissues of Swiss outbred mice, we tested the kinetics of virus spread of SW13 cell-passaged and parental JEV in the more susceptible IFN-α-$R^{-/-}$ mouse after inoculation of 10^3 PFU into the footpad. Jn-infected mice showed viremia 1 day p.i., which increased to 4×10^7 PFU/ml at 4 days p.i. (Fig. 4C). High virus titers were also detected in the spleen 2, 3, and 4 days p.i. and in the liver 3 and 4 days p.i. (Fig. 4D), but these findings may be partly the result of blood contamination, since the organ titers were below or similar to those observed in the blood, with the exception of that in the spleen at 4 days p.i. Nevertheless, the progressive rise in viremia indicates that significant extraneural replication occurred after footpad inoculation and that progeny virus was seeded into the circulation at a faster rate than that at which it was removed by the reticuloendothelial system. In accord with this observation and in support of a role of the liver as a target organ for virus growth in this mouse strain is the sharp rise of virus titers in the liver between 2 and 4 days p.i. (from below the detection limit to 2×10^6 PFU/g) in the absence of a similar increase in viremia during the same time period. Virus was first detectable in the brain at 3 days p.i. and increased by more than 3 logs to $>10^9$ PFU/g at 4 days p.i. (Fig. 4D).

IFN-α-$R^{-/-}$ mice inoculated with Js1 did not show detectable virus at any time in the blood, spleen, liver, and brain,

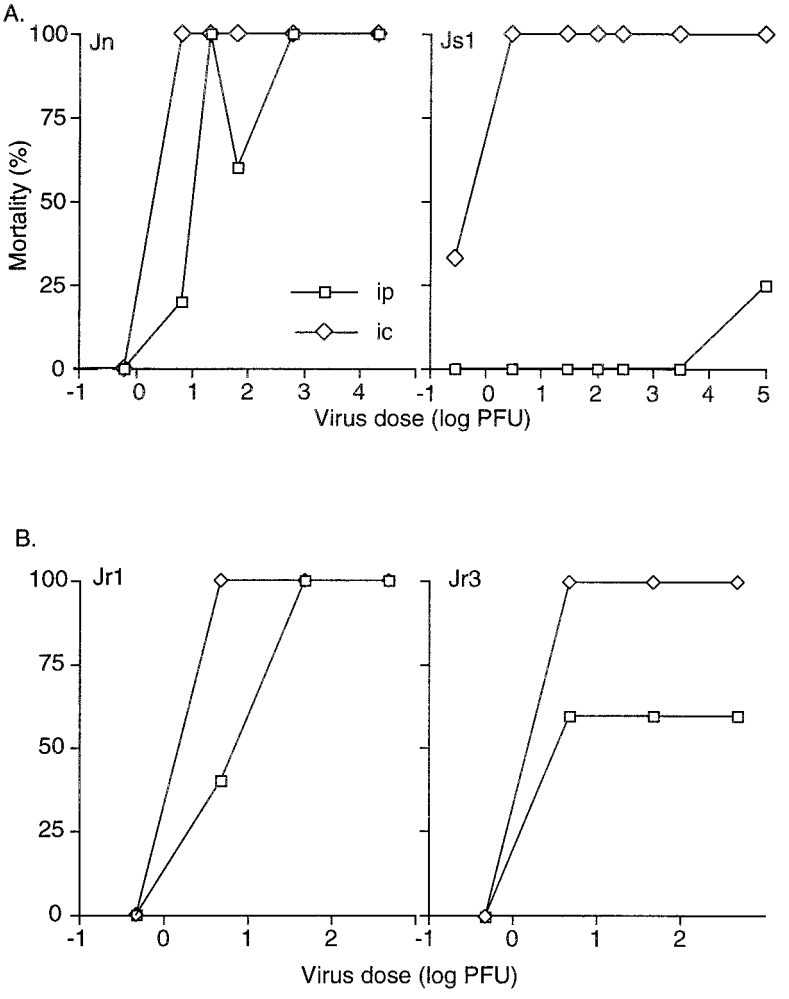

FIG. 3. Virulence of SW13 cell-passaged and parental JEV in 3-week-old Swiss outbred mice. Mortality in groups of five mice inoculated by the i.c. and i.p. routes with 10-fold serial dilutions of parental and SW13-cell passaged JEV (A) and revertants isolated from brain and liver (Jr1 and Jr3, respectively) (B) of IFN-α-$R^{-/-}$ mice infected with Js1.

based on infectivity titration (Fig. 4C and D) and RT-PCR performed with total infected cell RNA (detection limit, 10^4 RNA templates [data not shown]), suggesting a severe impediment in replication and/or virus spread from the extraneural site of inoculation of the attenuated virus.

Growth and tissue distribution of JEV and MVE isolates with distinct GAG-binding properties in IFN-α-$R^{-/-}$ mice after i.v. inoculation. The failure of SW13 cell-adapted JEV to spread from the site of footpad inoculation and to produce viremia and mortality in IFN-α-$R^{-/-}$ mice could have been due to a replication defect in extraneural tissues and/or the rapid removal of the variant virus from the circulation, thus preventing hematogenous spread. To further examine the mechanism of virulence attenuation, 6-week-old IFN-α-$R^{-/-}$ mice were inoculated i.v. with 10^5 PFU of Jn or Js, and virus titers in serum, spleen, liver, and brain were determined at 1, 2, and 4 days p.i. The parental Jn virus produced a fulminant infection; at 24 h p.i., viremia was already high (4×10^5 to 7×10^5 PFU/ml), and it remained high during the assay period with a peak titer at 2 days p.i. (Table 1). Virus titers in the spleen were consistently higher than those in the serum and peaked at 4 days p.i. ($\sim 10^7$ PFU/g), demonstrating efficient virus growth in this organ. At 4 days p.i., virus titers in the liver ($\sim 10^6$ PFU/g) and the brain ($\sim 10^9$ PFU/g) also exceeded that in the serum; however, this was not the case at the earlier time points (Table 1). Due to the high viremia and the inhibitory effect of liver and brain but not spleen homogenates on the infectivity of JEV (see below), it is not clear whether the kinetics of virus growth in the three organs differed.

In 6-week-old IFN-α-$R^{-/-}$ mice inoculated i.v. with 10^5 PFU of Js1, no detectable viremia was produced (Table 1). Relatively high virus titers were present in the spleen at 24 h p.i. in four animals tested (mean titer, 3×10^5 PFU/g). However, these titers declined on the following days and were reduced ≥1,000-fold at 4 days p.i. (Table 1), suggesting that the attenuated virus was cleared even in the absence of a functional IFN-α/β response. In some animals virus was also present in brain homogenates at 1 and 2 but not 4 days p.i. Interestingly, low Js titers ($\sim 10^3$ PFU/g) were seen in the livers of all animals between 1 and 4 days p.i. (Table 1). This could reflect a low level of virus growth in this organ or the deposition in the liver of virus released into the circulation from other sites of infection.

The kinetics of virus growth and tissue distribution of Js was

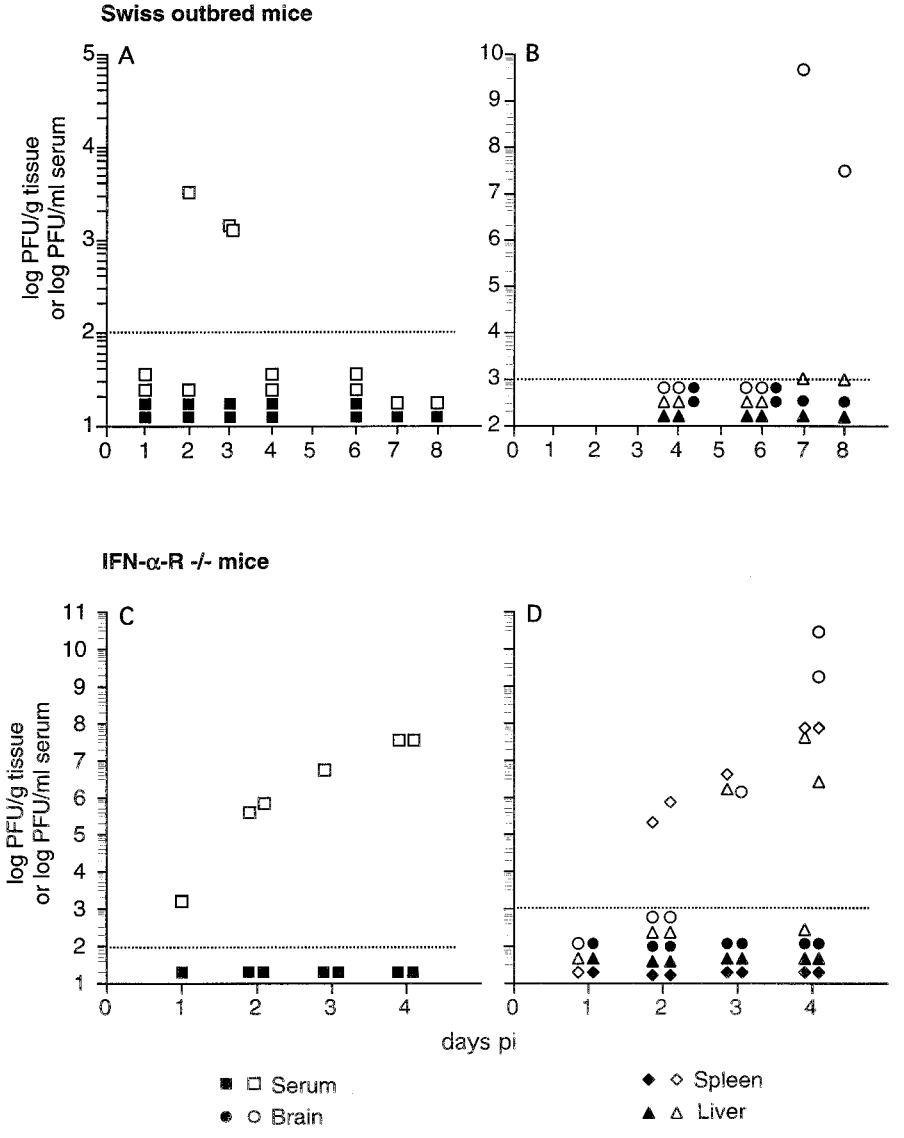

FIG. 4. Growth and tissue distribution of SW13 cell-passaged and parental JEV in mice after footpad inoculation. Virus titers in serum, brain, spleen and liver of 3-wk-old Swiss outbred (A and B) and IFN-α-$R^{-/-}$ (C and D) mice infected via the footpad with 10^3 PFU of Jn (open symbols) or Js1 (solid symbols).

also tested in 3-week-old IFN-α-$R^{-/-}$ mice infected with 10^5 PFU i.v. over a 4-day interval (Table 1). A low viremia was detected only at 2 days p.i. Virus titers in spleen and liver significantly exceeded those in the serum 2 and 4 days p.i. but declined over this time period. Given the low viremia, it is unlikely that virus detected in liver and spleen was due to blood contamination. In contrast to 3-week-old Swiss outbred and 6-week-old IFN-α-$R^{-/-}$ mice, Js was neuroinvasive in the 3-week-old knockout animals, in which virus titers in the brain rose to $>10^8$ PFU/g at 4 days p.i.

Effect of tissue homogenates on JEV infectivity. It should be noted that the low virus titers obtained for some organs, markedly the liver, significantly underestimate the true viral load due to the inhibitory effect of homogenates from some tissues on the infectivity of JEV (Table 2). The presence of ≥0.05% of liver homogenate derived from uninfected mice reduced the infectivity of Jn and Js viruses by >80%. Infectivity of Jn and Js viruses was reduced by >90% in the presence of ≥0.5% of brain homogenate. In contrast, serum did not reduce infectivity by more than 30% even at the highest concentration (5%) tested, and the spleen homogenate significantly reduced the infectivity of Jn and Js only at a concentration of ≥0.5% (Table 2). Thus, brain and spleen homogenates from infected tissues require $>10^2$-fold dilution, and infected liver homogenates require 10^3-fold dilution to obtain <50% reduction of JEV infectivity in plaque titrations of Vero cells.

Kinetics of blood clearance of JEV and MVE strains with distinct GAG-binding properties. Rapid removal of virus from the circulation by the reticuloendothelial system could account, at least in part, for poor virus growth in and inefficient spread from extraneural tissues and, in turn, loss of neuroinvasiveness of SW13 cell-passaged JEV and MVE. A faster

TABLE 1. Growth of SW13 cell-passaged and parental JEV in IFN-α-R$^{-/-}$ mice inoculated i.v. with 10^5 PFU

Mouse group and days p.i.	Virus titer[a] in:							
	Serum		Spleen		Liver[b]		Brain[b]	
	Jn	Js	Jn	Js	Jn	Js	Jn	Js
Six-week-old mice								
1	4×10^5	<100	5×10^5	8×10^5	1×10^3	2×10^3	2×10^3	1×10^3
	3×10^5	<100	7×10^5	1×10^5	1×10^4	2×10^3	2×10^3	1×10^3
	4×10^5	<100	7×10^5	7×10^4	2×10^4	2×10^3	5×10^3	$<1 \times 10^3$
	7×10^5	<100	1×10^6	2×10^5	5×10^4	2×10^3	1×10^4	$<1 \times 10^3$
2	2×10^6	<100	6×10^6	3×10^4	5×10^5	1×10^3	3×10^5	4×10^3
	5×10^6	<100	6×10^6	3×10^3	1×10^6	1×10^3	2×10^5	$<1 \times 10^3$
4	2×10^5	<100	2×10^7	$<1 \times 10^3$	2×10^6	1×10^3	2×10^9	$<1 \times 10^3$
	9×10^5	<100	1×10^7	3×10^3	2×10^6	1×10^3	2×10^9	$<1 \times 10^3$
Three-week-old mice								
1	NT[c]	<100	NT	NT	NT	NT	NT	NT
	NT	<100	NT	NT	NT	NT	NT	NT
2	NT	1×10^3	NT	9×10^6	NT	2×10^4	NT	3×10^3
	NT	400	NT	2×10^7	NT	3×10^4	NT	3×10^4
4	NT	<100	NT	4×10^5	NT	2×10^3	NT	7×10^8
	NT	<100	NT	7×10^4	NT	2×10^3	NT	1×10^8

[a] Virus titers in tissues from individual animals were determined by plaque formation on Vero cells and are expressed as PFU per gram of tissue or PFU per milliliter of serum.
[b] Virus titers may have been underestimated due to the inhibitory effect of tissue homogenates at low dilutions on plaque formation (see Table 2).
[c] NT, not tested.

kinetics of virus clearance from the circulation could be the function of increased affinity for GAGs during virus attachment and entry, as has been proposed for Venezuelan equine encephalitis and Sindbis viruses (1, 4). The rate of in vivo clearance of Jn and Js1 viruses from the circulation is shown in Fig. 5A. Mice were inoculated i.v. with 1.5×10^7 PFU of Jn or Js, and blood was collected at 5 and 30 min p.i. and assayed for infectious virus by plaque titration. In two animals inoculated with Jn, the reduction of viremia was <10-fold over the 30 min period. In contrast, viremia in animals inoculated with Js1 fell by >3 logs over the same period.

To test the generality of the more efficient removal of variants of encephalitic flaviviruses with high GAG-binding affinity, clearance from the circulation of attenuated variant MVE_{Ala390} was compared to that of parental virus MVE_{Asp390}. Variant MVE_{Ala390} has an Asp-to-Ala subsitution at residue 390 in E and shares phenotypic properties of virulence and GAG dependence similar to those of the MVE_{Gly390} and MVE_{His390} variants (13). Clearance of MVE_{Ala390} from the blood was significantly faster (15- to 45-fold reduction in viremia in 30 min) than that of MVE_{Asp390} which showed a <2-fold decrease in viremia during the 30-min interval (Fig. 5B).

To trace the organ distribution of JEV and MVE strains with different GAG-binding properties at an early time after removal from the circulation, gradient-purified, radioactively labeled virus was inoculated i.v., and blood, liver, spleen, kidney, and lung tissues were collected after 30 min for quantitation of virus by scintillation counting. Consistent with the rapid kinetics of blood clearance of SW13 cell-adapted variants shown in Fig. 5, >99.5% of infectious input virus was cleared from the blood for the attenuated variant MVE_{His390} at 30 min after i.v. infection, in comparison to ~75% blood clearance for

TABLE 2. Effect of tissue homogenates on JEV infectivity

Concn (%) of tissue homogenate[a]	% Inhibition[b] in:							
	Serum		Brain		Liver		Spleen	
	Jn	Js1	Jn	Js1	Jn	Js1	Jn	Js1
5	21	14	NT	NT	NT	NT	NT	NT
0.5	26	6	94	91	97	98	65	32
0.05	0	6	34	29	83	87	20	15
0.005	NT	NT	36	7	18	40	20	0

[a] Tissue homogenates were prepared in HBSS-BSA and mixed with ~100 PFU of virus at the concentrations indicated. Mixtures were held at room temperature for 15 min before they were assayed for infectivity in duplicates by plaque assay on Vero cells.
[b] Percent inhibition was calculated by using the following formula: [(1 − plaque numbers in virus-tissue homogenate mixture)/plaque numbers in controls] × 100. Controls were performed by mixing the virus with HBSS-BSA. NT, not tested.

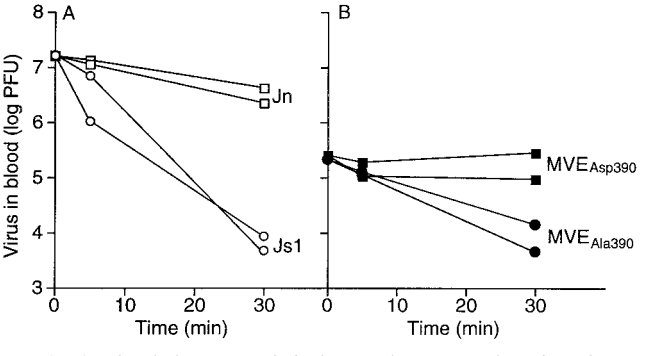

FIG. 5. Blood clearance of virulent and attenuated strains of JEV and MVE with distinct GAG-binding properties. Eight-week-old Swiss outbred mice were inoculated i.v. in groups of two with Jn (□; 1.7×10^7 PFU) or Js1 (○; 1.6×10^7 PFU) (A) and MVE_{Asp390} (■; 2.4×10^5 PFU) or MVE_{Gly390} (●; 2.0×10^5 PFU) (B). At 5 and 30 min p.i., blood was collected, virus titers were determined by plaque assay of Vero cell monolayers, and titers were multiplied by an estimate of the blood volume for each animal.

TABLE 3. Organ distribution of radiolabeled virulent MVE_{Asp390} and attenuated MVE_{His390} at 30 min after i.v. inoculation[a]

Mouse	% cpm of input								Infectivity	
	Liver		Spleen		Lungs		Kidneys		Blood	
	Asp_{390}	His_{390}	Asp_{390}	His_{390}	Asp_{390}	His_{390}	Asp_{390}	His_{390}	Asp_{390}	His_{390}
1	5.6	12.0	0.3	1.0	0.4	0.7	0.5	1.0	27	<0.5
2	5.8	12.0	0.4	1.7	0.5	0.7	0.5	1.0	22	<0.5

[a] Six-week-old C57BL/6 mice were inoculated i.v. with ^{35}S-labeled MVE_{Asp390} (7.2×10^4 cpm; 4×10^7 PFU) or MVE_{His390} (4.6×10^4 cpm; 6×10^5 PFU), and the livers, spleens, lungs, and kidneys were collected at 30 min p.i. for determination of virus load by scintillation counting. Blood was collected at the same time for determination of infectivity by plaque titration. Values are given as a percentage of input radioactivity or infectivity.

the parent MVE_{Asp390} virus (Table 3). The organ distribution of the MVE_{Asp390}-specific radioactivity at 30 min after inoculation showed that spleen, lung, and kidney contained <0.5% of input counts and that 5.6 to 5.8% of counts were accumulated in the liver (Table 3). A two- to threefold-greater recovery of input radioactivity was found in the organs of mice inoculated with MVE_{His390} with a relative distribution comparable to that of MVE_{Asp390}.

Reversion of virulence and heparin-sensitivity of attenuated JEV variants. Virus recovered from the brain, spleen, and liver of 3-week-old IFN-α-$R^{-/-}$ mice inoculated with SW13 cell-passaged Js1 virus contained a mixed population of large (>3-mm) and small (~0.5-mm) plaques, in contrast to the exclusively small plaque phenotype observed for the virus stock used for inoculation. Given the correlation between plaque size and GAG-binding properties, we tested whether the emerging large plaque isolates were revertants with respect to heparin sensitivity and virulence and determined the corresponding genetic changes. Two large plaques were isolated from Vero cell monolayers infected with brain homogenate from a Js1-infected IFN-α-$R^{-/-}$ mouse at 4 days p.i. and then amplified by one passage on Vero cells. Similarly, two large plaques, as well as a small plaque, were isolated and amplified from cells infected with spleen or liver homogenates obtained from different Js1-infected mice at 4 and 2 days p.i., respectively (Table 4). The resultant virus stocks showed uniform plaque size when titrated on Vero cells under agar overlay (Table 4). When the large plaque isolates Jr1, Jr3, and Jr6 from the brain, liver, and spleen, respectively, were tested for the inhibition of infectivity by heparin, all three showed a susceptibility to heparin similar to that of the Jn virus (Table 4). Jr1 and Jr3 were examined for mouse virulence as described above for Jn and Js1 viruses (Fig. 3B). Jr1 had fully regained neuroinvasiveness in 3-week-old Swiss outbred mice, whereas Jr3 was only partially neuroinvasive, producing ≤60% mortality even at the highest dose of virus inoculum given i.p.

The nucleotide sequences corresponding to the prM and E protein genes were determined for the parental Jn, SW13 cell-passaged Js1, and the plaque size revertants isolated from various tissues of Js1-infected mice (Table 4). Jn and Js1 differed at a single nucleotide (nt 1893), which gave rise to a nonconservative amino acid substitution at E protein residue 306 (Glu to Lys; Table 4). In all revertants giving rise to large plaques, changes were found in the E protein at or close to residue 306. In Jr1, Jr2, Jr6, and Jr7, which were isolated from brain and spleen tissues, the codon for Lys_{306} was mutated back to that for Glu; thus, the nucleotide sequence was reverted to that of the Jn virus. In Jr3 and Jr4, which were isolated from liver, the codon for Lys_{307} was mutated to that of Glu, while the codon for Lys_{306} was retained. There were also additional silent nucleotide changes in the E protein gene of the large plaque isolates Jr 3, Jr4, Jr6, and Jr7 derived from the liver or spleen (Table 4). Notably, two small plaques isolated from liver and spleen (Jr5 and Jr8, respectively) were identical in sequence to the Js1 virus in the E gene. Direct sequence analysis performed with total RNA extracted from the same

TABLE 4. Phenotypic and genotypic properties of JEV variants

Virus	Plaque size[a]	Isolation parameters			Change in E gene[b]	Change in E protein	Heparin sensitivity[c]	Neuroinvasiveness
		Days p.i.	Mouse	Tissue				
Jn	Large	NA[d]	NA	NA	NC	NC	No	High
Js1	Small	NA	NA	NA	1893G→A	306 E→K	Yes	Low
Jr1	Large	4	C	Brain	NC	NC	No	High
Jr2	Large	4	C	Brain	NC	NC	NT[f]	NT
Jr3	Large	2	A	Liver	1896A→G, 2364C→T[e]	307 K→E	No	Intermediate
Jr4	Large	2	A	Liver	1896A→G, 2364C→T[e]	307 K→E	NT	NT
Jr5	Small	2	B	Liver	1893G→A	306 E→K	Yes	NT
Jr6	Large	4	D	Spleen	1757A→G[e]	NC	No	NT
Jr7	Large	4	D	Spleen	1757A→G[e]	NC	NT	NT
Jr8	Small	4	D	Spleen	1893G→A	306 E→K	Yes	NT

[a] Plaque size on Vero cell monolayers: large, ~3 mm; small, ~0.5 mm.
[b] No nucleotide differences were found in the M protein gene. NC, no change from Nakayama sequence.
[c] Inhibition of plaque formation in BHK-21 cells by heparin (200 μg/ml). No, inhibition of < 30%; yes, inhibition of >80%.
[d] NA, not applicable.
[e] Silent nucleotide change.
[f] NT, not tested.

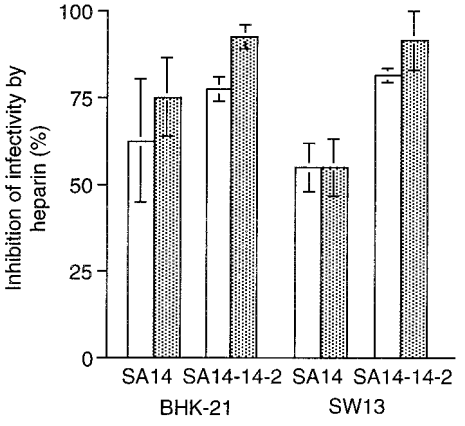

FIG. 6. Inhibition by heparin of infectivity of virulent JEV SA14 and its vaccine derivative SA14-14-2. Inhibition of virus infectivity in the presence of 50 (open bars) and 200 (shaded bars) μg of heparin/ml was determined as described in the legend to Fig. 1. The error bars show the standard deviation values of each set of duplicates.

brain and spleen homogenates used for isolation of plaque size revertants showed no sign of the revertants, indicating that these were a small minority, a finding consistent with the low abundance (<1%) of large plaques obtained from the tissues. In contrast, sequence analysis of total RNA extracted from liver of two animals at 2 days p.i. showed that the pseudorevertant virus with an additional change (Glu_{307}) in E was predominant in one animal (mouse A, Table 4), but there was no sign of the Glu_{307} revertant in the liver of a second mouse (mouse B, Table 4).

Heparin sensitivity of the virulent JEV SA14 and its vaccine derivative SA14-14-2. The association of virulence attenuation with heparin sensitivity was also examined for the JEV live-attenuated vaccine, SA14-14-2, in comparison to the virulent parental virus, SA14. The vaccine strain showed greater susceptibility to heparin inhibition of virus infectivity on SW13 cell monolayers than the parental virus at two heparin concentrations (50 and 200 μg/ml) tested, with only a marginal difference in heparin inhibition seen on BHK cells (Fig. 6).

DISCUSSION

This study reports on the generation of attenuated variants of JEV by host cell adaptation and defines a molecular determinant and in vivo mechanism for the loss of the capacity of the JEV and MVE variants to produce disease in a mouse model of flavivirus encephalitis. The rapid selection of mutants with altered growth and virulence phenotypes by serial virus passage in the human adenocarcinoma cell line, SW13, was first demonstrated for MVE (17). The MVE variants were altered in their cell attachment and entry properties, which was reflected in an increased susceptibility to the inhibitory effect of heparin on infectivity (13) and an enhanced binding affinity, in vitro, to GAGs (shown here). SW13 cell-adapted JEV variants closely resembled the MVE variants in growth, heparin sensitivity, and GAG-binding phenotypes. Accordingly, it appears that the two closely related flaviviruses utilize identical alternative entry mechanisms for the infection of SW13 cells; this mechanism most likely involves an increased dependence on cell surface GAGs. A reliable marker for the phenotypic changes associated with the adaptation of the JEV serocomplex flaviviruses to growth in SW13 cells was that of a small plaque phenotype on Vero and SW13 cell monolayers, highlighting the simplicity of the selection procedure. The small plaque phenotype of heparan sulfate-binding virus variants is thought to reflect their greater sensitivity to the inhibitory effect on virus growth of sulfate impurities in the agar overlay (34).

Virulence attenuation of SW13 cell-adapted JEV variants was, like that of the MVE variants (13, 17), predominantly the result of a loss of neuroinvasiveness. This conclusion is based on (i) comparative i.p. and i.c. LD_{50} determinations for 3-week-old Swiss outbred mice, which differed by more than 3 orders of magnitude for the passage variants but less than 10-fold for the parent virus; (ii) the inability of the passage variants to enter the brain after footpad inoculations into 3-week-old Swiss outbred and IFN-α-$R^{-/-}$ mice, in contrast to the parent virus which was neuroinvasive; and (iii) the resistance of 6-week-old IFN-α-$R^{-/-}$ mice to i.v. infection with a high virus dose of SW13 cell-adapted JEV, in contrast to the widely disseminating and uniformly lethal infections elicited by the parental virus in these animals. The mechanism by which encephalitic flaviviruses breach the blood-brain barrier to enter the brain parenchyma remains uncertain. Candidate routes for central nervous system invasion include (11), although not exclusively: infection of peripheral nerves or olfactory neurons unprotected by the blood-brain barrier (23, 25); infection of vascular endothelial cells of capillaries in the brain, transcytosis, and release of virus into the brain parenchyma (15); and diffusion of virus between capillary endothelial cells into the brain parenchyma (12, 18). A key factor for neuroinvasion by these means, but in particular the latter two mechanisms, is the capacity of neurotropic flaviviruses to generate high titers and persistent viremia.

A striking finding in this study was the 20- to 100-fold-faster kinetics of blood clearance of the attenuated MVE and JEV variants, respectively, relative to the parental viruses. Given that the physical nature of the virion surface impacts significantly on blood clearance, we propose that the increased affinity to GAGs of the SW13 cell-adapted variants was responsible for their rapid removal from the bloodstream. The possibility that differential aggregation of virus particles for the various strains of MVE and JEV accounts for altered clearance kinetics can be excluded, since infectious titers remained unchanged during handling and storage of virus stocks and the sedimentation properties through the sucrose gradient were similar between the GAG-binding variant and the parental virus. The faster kinetics of virus clearance from the circulation was reflected in a two- to threefold-increased deposition of radiolabeled variant virus in various organs (liver, spleen, lung, and kidney) at 30 min after injection, relative to the parental virus. However, relatively little input virus was recovered from the organs, probably as a consequence of the ubiquitous distribution of GAGs on the cell surface and in the extracellular matrix (31). Hence, both the passaged and parent viruses would become widely distributed in the animal, probably by adherence to capillary endothelial cells as they are removed from the bloodstream. However, some accumulation of virus was found in the liver, either due to the anatomy of this organ

or to the enrichment of the liver with GAGs, which are at the most sulfated end of the heparan sulfate spectrum (19).

The SW13 cell-passaged variants were severely limited in their capacity to spread in the animal after peripheral inoculation. Injection into the footpad gave no detectable virus in the blood and tissues examined, indicating that the variants failed to exit from the inoculation site via the efferent lymphatic. Low virus titers of the passaged variants were also seen in various organs after i.v. inoculation of 10^5 PFU into 6-week-old IFN-α-$R^{-/-}$ mice, despite the wide organ and tissue deposition of virus in the inoculum achieved by this route. This finding contrasts with the fulminating, lethal infection produced by the parental JEV in these animals. Although a restriction in the ability of the SW13-passaged flavivirus variants to grow in mouse tissues was not excluded in this study, a number of findings suggest that the variants were not significantly limited in growth: (i) the variants produced progeny virus titers of comparable magnitude to that of the parent viruses in infected cell cultures (data not shown), (ii) the variants grew to high titers in the brains of 3-week-old i.c.-inoculated Swiss outbred mice and i.v.-inoculated IFN-α-$R^{-/-}$ mice, and (iii) the growth of the variants was clearly apparent in spleens of 3- and 6-week-old IFN-α-$R^{-/-}$ mice in the first 2 days after i.v. infection, despite low or absent viremia, but thereafter declined. The strong adherence of the GAG-binding variants to proteoglycans on cell surface and intercellular matrix should also not be overlooked, since it may adversely impact on their ability to disseminate and also on the detection of progeny virus in tissue homogenates.

Despite the apparent ability of the passage variants to grow in extraneural tissues and in the brain, they had a largely diminished capacity to enter the central nervous system after extraneural infection. The crucial factor in virulence attenuation of the GAG-binding variants was their inability to produce viremia of sufficient magnitude and/or duration required for brain invasion. Two factors determine the magnitude of the viremia: the amount of virus entering the blood and the efficiency with which it is removed by the reticuloendothelial system. We could demonstrate that the attenuated variants were cleared from the blood with significantly faster kinetics than those of the virulent parental viruses. The possibility that the increased affinity of the variants for GAGs prevented efficient entry of progeny virus into the bloodstream remains but is difficult to test experimentally. This mechanism of attenuation for JEV serocomplex flaviviruses closely resembles that proposed for alphavirus variants that bind strongly to GAGs (1, 4).

IFN-α-$R^{-/-}$ mice were highly susceptible to infection with JEV serotype flaviviruses. While viremia and virus titers in extraneural issues can rarely be detected in laboratory mice older than 3 to 4 weeks of age (10), 6-week-old IFN-α-$R^{-/-}$ mice infected with JEV and MVE (this study and unpublished results) showed early, high, and persistent viremia, rising virus titers in all tissues examined, and 100% mortality by day 6 p.i. This confirms the importance of IFN-α/β in the resistance of mice to infection with encephalitic flaviviruses. Interestingly, a comparison of the susceptibility of 3- and 6-week-old IFN-α-$R^{-/-}$ mice to i.v. infection with a GAG-binding JEV variant showed significantly higher virus titers in spleen, liver, and brain of the younger animals, suggesting that factors other than the IFN-α/β response contribute to the age-dependent resistance of mice to flavivirus infection.

The most likely molecular basis for virulence attenuation of the SW13 cell-passaged JEV variants was a single amino acid substitution at residue 306 in the E protein (Glu_{306} to Lys). The substitution gave rise to an increase in net positive charge on the E protein, a finding consistent with the role of basic amino acid motifs in virus attachment to negatively charged heparan sulfate (31). GAG-binding variants of MVE selected by passage in SW13 cells were also mutated exclusively at a single residue on the E protein (Asp_{390}) and displayed an increase in net positive charge on the virion surface (17). Residue Asp_{390} is part of a RGD integrin-binding motif present in the putative receptor-binding domain on the MVE E protein (17) Given the close genetic relatedness of MVE and JEV (82% amino acid sequence homology in the E protein) and the conservation of the RGD motif in JEV, it is of interest that an alternative site was involved in the adaptation of JEV to growth in SW13 cells. However, by analogy with the crystal structure of the tick-borne encephalitis virus E protein (29), it is predicted that JEV E protein residue 306 is found on a surface exposed region (Ax-A loop), directly opposing residue 390 located in an adjacent (FG) loop. This spatial proximity of residues 306 and 390 strongly suggests that the three-dimensional structure comprising the two loops at the lateral surface of the E protein constitutes an important GAG-binding site functioning in the attachment and entry of the JEV serotype flaviviruses.

Growth of the GAG-binding variant of JEV in IFN-α-$R^{-/-}$ mice yielded revertants with a characteristic large plaque phenotype; however, the ratio of revertant to nonrevertant phenotypes remained low (<10% on the basis of plaque size) in the brain and spleen, indicating that the pathogenesis in these animals was due to growth of the attenuated virus rather than that of the revertant virus. Revertants with an amino acid change at E protein residue 306 were isolated from the spleens and brains of infected mice. This reversion restored the E protein sequence and, in turn, virulence and GAG-binding properties to that of the Nakayama strain and supports our conclusion that the phenotypic differences of the passage variants from that of the parental virus resulted from the single amino acid substitution at Asp_{306} in the E protein. Pseudorevertants with a charge substitution at E protein residue 307 (Lys_{307} to Asp) were isolated from the liver of one infected animal. This virus was comparable to the virulent Nakayama strain in the sensitivity to inhibition of infectivity by heparin but could be distinguished from it by an only partial reversion to neuroinvasiveness. The possibility that the pseudoreversion reflects an adaptation to growth in hepatocytes was not addressed.

Finally, we show that the JEV vaccine SA14-14-2 was, similar to the SW13 cell-passaged variants of JEV, more sensitive to the inhibitory effect of heparin on virus infectivity than virulent JEV. Accordingly, it is likely that a rapid clearance from the circulation and a deficiency in its capacity to spread from extraneural sites of infection are also important factors in the in vivo mechanism for virulence attenuation of the vaccine strain. SA14-14-2 differs from its parent virus (JEV SA14) at 5 amino acids in the E protein and 10 elsewhere (27, 28). Several studies have shown that a Glu_{138}-to-Lys substitution in the

JEV E protein, which is one of the five differences, correlates with small plaque morphology, increased sensitivity to inhibition of plaque formation by heparin and dextran sulfate, loss of neuroinvasiveness and neurovirulence, and increased liver tropism (5, 32, 33). Residues 138 and 306 are predicted to be located at distant sites on the E protein in domains II and III, respectively (29). Thus, distinct regions in the flavivirus E protein can apparently contribute to the viral GAG-binding phenotype, an observation which was also made in a study on tick-borne encephalitis virus (21). It is therefore puzzling that host cell adaptation of JEV serocomplex flaviviruses to SW13 cells exclusively selected for amino acid substitutions in surface-exposed loops in domain III of the E protein; it would be of interest to explore whether flavivirus infection of this cell type involves a distinctive receptor usage or entry mechanism.

ACKNOWLEDGMENT

We thank Roy Hall for providing the JEV strains SA14 and SA14-14-2.

REFERENCES

1. **Bernard, K. A., W. B. Klimstra, and R. E. Johnston.** 2000. Mutations in the E2 glycoprotein of Venezuelan equine encephalitis virus confer heparan sulfate interaction, low morbidity, and rapid clearance from blood of mice. Virology **276:**93–103.
2. **Bernfield, M., M. Gotte, P. W. Park, O. Reizes, M. L. Fitzgerald, J. Lincecum, and M. Zako.** 1999. Functions of cell surface heparan sulfate proteoglycans. Annu. Rev. Biochem. **68:**729–777.
3. **Burke, D. S., and T. P. Monath.** 2001. Flaviviruses, p. 1043–1126. *In* B. N. Fields, D. M. Knipe, and P. M. Howley (ed.), Fields virology, 4th ed. Lippincott/Williams & Wilkins, Philadelphia, Pa.
4. **Byrnes, A. P., and D. E. Griffin.** 2000. Large-plaque mutants of Sindbis virus show reduced binding to heparan sulfate, heightened viremia, and slower clearance from the circulation. J. Virol. **74:**644–651.
5. **Chen, L. K., Y. L. Lin, C. L. Liao, C. G. Lin, Y. L. Huang, C. T. Yeh, S. C. Lai, J. T. Jan, and C. Chin.** 1996. Generation and characterization of organtropism mutants of Japanese encephalitis virus in vivo and in vitro. Virology **223:**79–88.
6. **De Madrid, A. T., and J. S. Porterfield.** 1974. The flaviviruses (group B arboviruses): cross-neutralization study. J. Gen. Virol. **23:**91–96.
7. **Eldadah, A. H., N. Nathanson, and R. Sarsitis.** 1967. Pathogenesis of West Nile Virus encephalitis in mice and rats. 1. Influence of age and species on mortality and infection. Am. J. Epidemiol. **86:**765–775.
8. **Grossberg, S. E., and W. F. Scherer.** 1966. The effect of host age, virus dose and route of inoculation on inapparent infection in mice with Japanese encephalitis virus. Proc. Soc. Exp. Biol. Med. **123:**118–124.
9. **Hahn, C. S., J. M. Dalrymple, J. H. Strauss, and C. M. Rice.** 1987. Comparison of the virulent Asibi strain of yellow fever virus with the 17D vaccine strain derived from it. Proc. Natl. Acad. Sci. USA **84:**2019–2023.
10. **Huang, C. H., and C. Wong.** 1963. Relation of the peripheral multiplication of Japanese B encephalitis virus to the pathogenesis of the infection in mice. Acta Virol. **7:**322–330.
11. **Johnson, R. T., and G. A. Mims.** 1968. Pathogenesis for viral infections of the nervous system. N. Engl. J. Med. **278:**84–92.
12. **Kobiler, D., S. Lustig, Y. Gozes, D. Ben-Nathan, and Y. Akov.** 1989. Sodium dodecyl sulphate induces a breach in the blood-brain barrier and enables a West Nile virus variant to penetrate into mouse brain. Brain Res. **496:**314–316.
13. **Lee, E., and M. Lobigs.** 2000. Substitutions at the putative receptor-binding site of an encephalitic flavivirus alter virulence and host cell tropism and reveal a role for glycosaminoglycans in entry. J. Virol. **74:**8867–8875.
14. **Lee, E., C. E. Stocks, S. M. Amberg, C. M. Rice, and M. Lobigs.** 2000. Mutagenesis of the signal sequence of yellow fever virus prM protein: enhancement of signalase cleavage in vitro is lethal for virus production. J. Virol. **74:**24–32.
15. **Liou, M. L., and C. Y. Hsu.** 1998. Japanese encephalitis virus is transported across the cerebral blood vessels by endocytosis in mouse brain. Cell Tissue Res. **293:**389–394.
16. **Lobigs, M., I. D. Marshall, R. C. Weir, and L. Dalgarno.** 1986. Genetic differentiation of Murray Valley encephalitis virus in Australia and Papua New Guinea. Aust. J. Exp. Biol. Med. Sci. **64:**571–585.
17. **Lobigs, M., R. Usha, A. Nestorowicz, I. D. Marshall, R. C. Weir, and L. Dalgarno.** 1990. Host cell selection of Murray Valley encephalitis virus variants altered at an RGD sequence in the envelope protein and in mouse virulence. Virology **176:**587–595.
18. **Lustig, S., H. D. Danenberg, Y. Kafri, D. Kobiler, and D. Ben-Nathan.** 1992. Viral neuroinvasion and encephalitis induced by lipopolysaccharide and its mediators. J. Exp. Med. **176:**707–712.
19. **Lyon, M., J. A. Deakin, and J. T. Gallagher.** 1994. Liver heparan sulfate structure. A novel molecular design. J. Biol. Chem. **269:**11208–11215.
20. **MacDonald, F.** 1952. Murray Valley encephalitis infection in the laboratory mouse. I. Influence of age on the susceptibility of infection. Aust. J. Exp. Biol. Med. Sci. **30:**319–324.
21. **Mandl, C. W., H. Kroschewski, S. L. Allison, R. Kofler, H. Holzmann, T. Meixner, and F. X. Heinz.** 2001. Adaptation of tick-borne encephalitis virus to BHK-21 cells results in the formation of multiple heparan sulfate binding sites in the envelope protein and attenuation in vivo. J. Virol. **75:**5627–5637.
22. **McAda, P. C., P. W. Mason, C. S. Schmaljohn, J. M. Dalrymple, T. L. Mason, and M. J. Fournier.** 1987. Partial nucleotide sequence of the Japanese encephalitis virus genome. Virology **158:**348–360.
23. **McMinn, P. C., L. Dalgarno, and R. C. Weir.** 1996. A comparison of the spread of Murray Valley encephalitis viruses of high or low neuroinvasiveness in the tissues of Swiss mice after peripheral inoculation. Virology **220:**414–423.
24. **Monath, T. P., C. B. Cropp, G. S. Bowen, G. E. Kemp, C. J. Mitchell, and J. J. Gardner.** 1980. Variation in virulence for mice and rhesus monkeys among St. Louis encephalitis virus strains of different origin. Am. J. Trop. Med. Hyg. **29:**948–962.
25. **Monath, T. P., C. B. Cropp, and A. K. Harrison.** 1983. Mode of entry of a neurotropic arbovirus into the central nervous system. Reinvestigation of an old controversy. Lab. Investig. **48:**399–410.
26. **Müller, U., U. Steinhoff, L. F. Reis, S. Hemmi, J. Pavlovic, R. M. Zinkernagel, and M. Aguet.** 1994. Functional role of type I and type II interferons in antiviral defense. Science **264:**1918–1921.
27. **Ni, H., G. J. Chang, H. Xie, D. W. Trent, and A. D. Barrett.** 1995. Molecular basis of attenuation of neurovirulence of wild-type Japanese encephalitis virus strain SA14. J. Gen. Virol. **76:**409–413.
28. **Nitayaphan, S., J. A. Grant, G. J. Chang, and D. W. Trent.** 1990. Nucleotide sequence of the virulent SA-14 strain of Japanese encephalitis virus and its attenuated vaccine derivative, SA-14-14-2. Virology **177:**541–552.
29. **Rey, F. A., F. X. Heinz, C. Mandl, C. Kunz, and S. C. Harrison.** 1995. The envelope glycoprotein from tick-borne encephalitis virus at 2 Å resolution. Nature **375:**291–298.
30. **Rice, C. M., E. M. Lenches, S. R. Eddy, S. J. Shin, R. L. Sheets, and J. H. Strauss.** 1985. Nucleotide sequence of yellow fever virus: implications for flavivirus gene expression and evolution. Science **229:**726–733.
31. **Rostand, K. S., and J. D. Esko.** 1997. Microbial adherence to and invasion through proteoglycans. Infect. Immun. **65:**1–8.
32. **Su, C. M., C. L. Liao, Y. L. Lee, and Y. L. Lin.** 2001. Highly sulfated forms of heparin sulfate are involved in Japanese encephalitis virus infection. Virology **286:**206–215.
33. **Sumiyoshi, H., G. H. Tignor, and R. E. Shope.** 1995. Characterization of a highly attenuated Japanese encephalitis virus generated from molecularly cloned cDNA. J. Infect. Dis. **171:**1144–1151.
34. **Takemoto, K. K.** 1966. Plaque mutants of animal viruses. Prog. Med. Virol. **8:**314–348.
35. **Tyler, K. N., and N. Nathanson.** 2001. Pathogenesis of viral infections, p. 199–244. *In* B. N. Fields, D. M. Knipe, and P. M. Howley (ed.), Fields virology, 4th ed. Lippincott/Williams & Wilkins, Philadelphia, Pa.
36. **Xie, W. Q., and L. I. Rothblum.** 1991. Rapid, small-scale RNA isolation from tissue culture cells. BioTechniques **11:**324–327.